DESIGN AND MODELING OF A PLASMA REACTOR FOR THE PRODUCTION OF O_2 FROM THE CONVERSION OF CO_2

Inês Robalo Dias Martins dos Santos

Supervisors:
Prof. Nuno Pinhão
Prof. Pedro Viegas

A special thanks to Prof. Marta Dias for her continuous cooperation in the development of MIEC membranes.

Campus Tecnológico e Nuclear – IST ***MEFT 2025/2026***

Introduction

Driven by the need to valorize CO_2 as a resource rather than a waste, this project develops a compact DBD plasma reactor that combines non-thermal plasma CO_2 dissociation with mixed ionic–electronic conducting (MIEC) membranes for selective oxygen separation, which are temperature activated at 700-800 °C .Multiphysics simulation guides reactor modeling and optimization, while perovskite-based MIEC membranes of $\mathbf{Ba_{0.5}Sr_{0.5}Co_{0.8}Fe_{0.2}O_{3-\delta}}$ (BSCF) are synthesized and tested for oxygen permeability and stability under CO_2 exposure. The integrated system should enable scalable, energy-efficient oxygen production from CO_2, with applications in Mars in-situ resource utilization and low-carbon terrestrial O_2 generation.

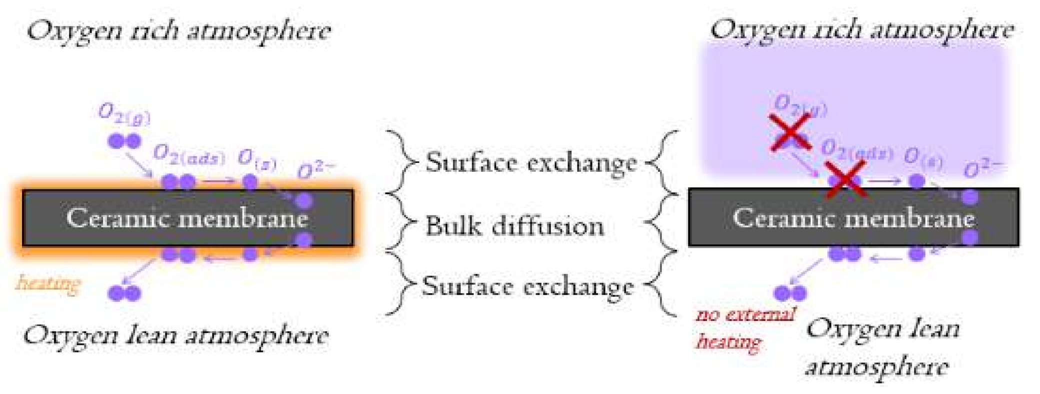

Figure 1 – MIEC membrane operation, and oxygen transport mechanisms [1].

Numerical modeling

Numerical modeling is performed to evaluate temperature distribution, electric field distribution, gas flow and mechanical stress across reactor components. The reactor geometry was meshed using **Gmsh** to create detailed 2D and 3D models, which are then used for finite element simulations, using **Elmer FEM** software. This approach informed decisions on sizing, boundary conditions, and material selection for the plasma reactor.

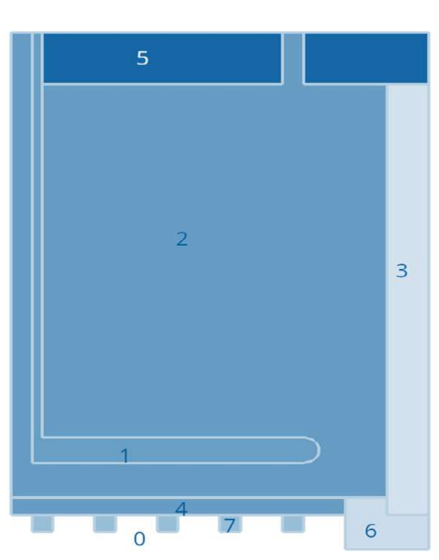

Reactor elements:
0 = Vacuum
1 = Electrode (stainless steel)
2 = Gas (CO_2)
3 = Quartz (fused silica)
4 = Ceramic membrane (BSCF)
5 = Lid (MACOR)
6 = Membrane support (MACOR)
7 = Heater (Inconel 600)
Mesh step: 0.125 mm

Figure 4 - 2D axi-symmetric reactor model, and composition.

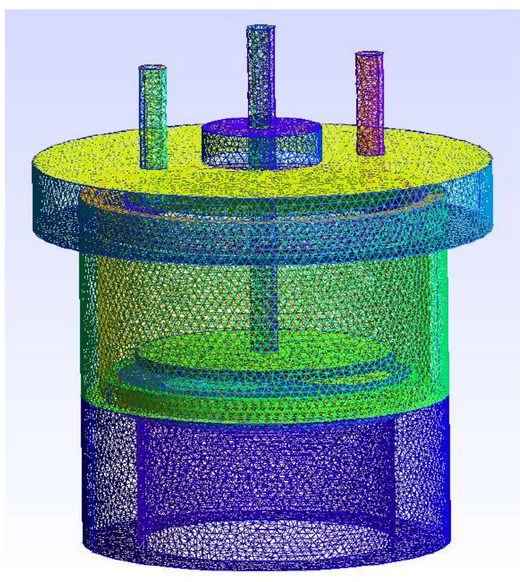

Figure 5 – 3D reactor model.

Simulations in Elmer GUI incorporate solid and gaseous **heat transfer equations, electrostatics, Navier–Stokes equations for gas flow, and displacement coupled with von Mises stress analysis** to account for thermal expansion effects within the reactor components. **ParaView** is the chosen software to visualize the results of the numerical model.

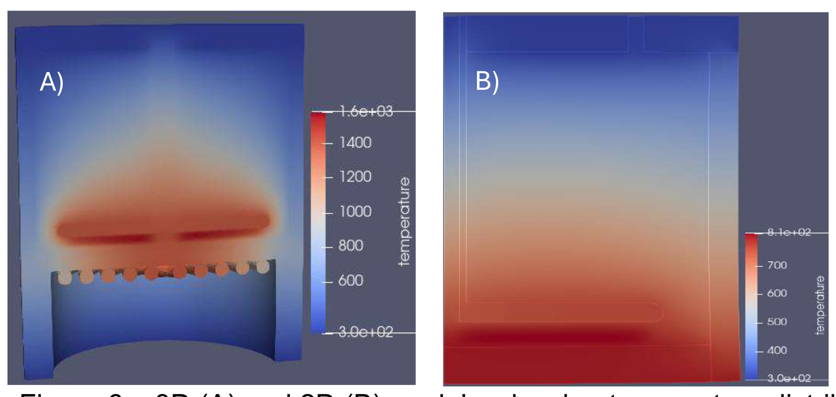
Figure 6 – 3D (A) and 2D (B) models, showing temperature distribution (K) for a 8 W heating power.

All practical reactor properties are simulated using Elmer GUI calculations and ParaView graphing software.

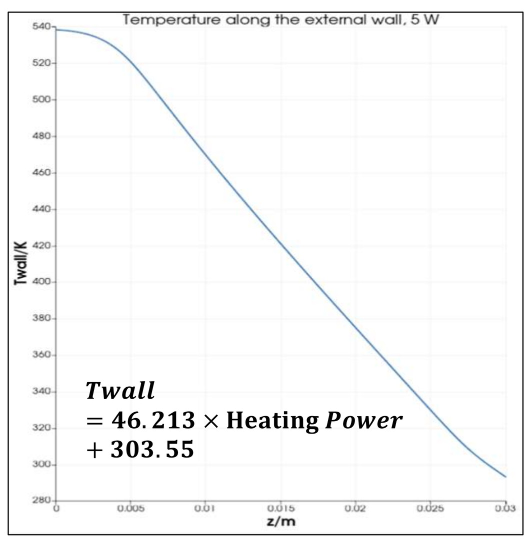

Figure 9 – Linear decrease of the temperature along the external wall of the reactor, at a heating power of 5 W.

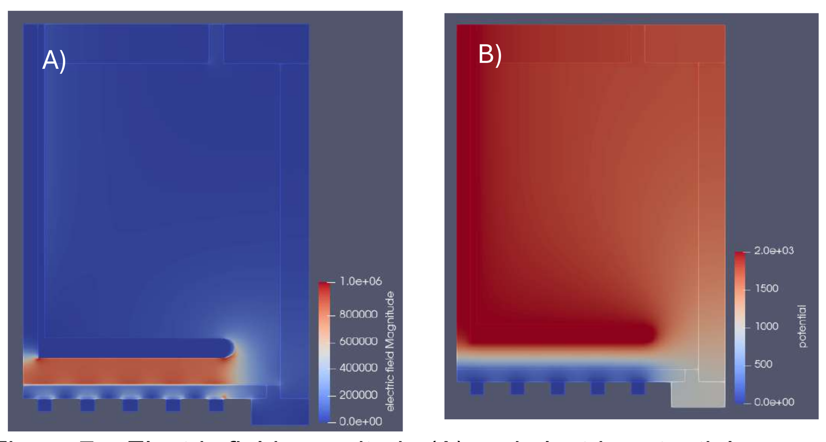
Figure 7 – Electric field magnitude (A) and electric potential distribution (B) for the 2D simulation, at an applied voltage of 2 kV

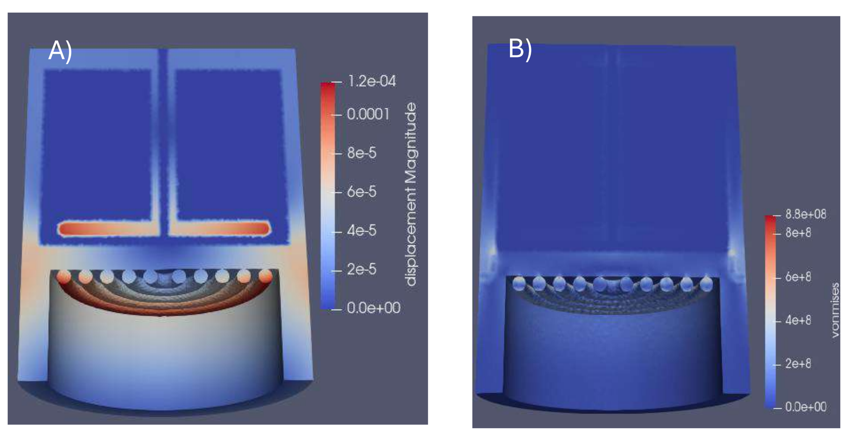
Figure 8 – Linear displacement (A) and Von-misses analysis (B) for the 3D simulation, indicating heat expansion.

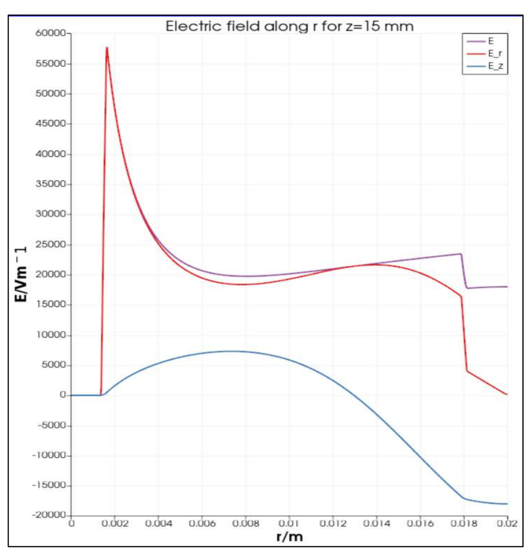
Figure 10 – 2D results for electric field components along the radius for z = 15 mm, with an applied voltage of 2 kV.

Experimental methods

BSCF membranes are developed from a commercially obtained oxide powder, which is milled and calcined at 900 °C for 4 h, leading to the formation of a perovskite structure. Samples are developed through different methods:

- Using a uniaxial pressure of 200 MPa, followed by a heat treatment in the oven, from 15 h to 30 h, using temperatures of 700-1000°C ;
- By employing a binder/dispersant mixture of ethylcellulose and terpineol, at a ratio of 1:10 [3].

Samples are analysed using SEM and XRD, for in-depth analysis of structural and chemical status.

Figure 2– BSCF perovskite (ABO_3) structure [2].

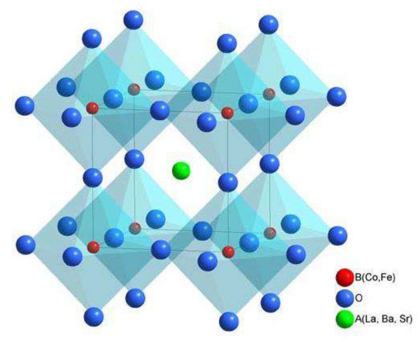


Figure 3 – Mold used to produce ethylcellulose/terpineol BSCF samples.

Results

Resulting BSCF pellets all displayed fractures in the radial direction ⟶ **Improper thermal profile? Insufficient or inadequate pressurization?**

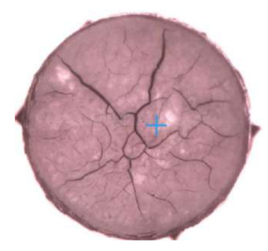

- Fusion occurred at 1250 °C, which is confirmed using a DTA analysis of the BSCF sample;
- XRD patterns of BSCF samples, and of the BSCF powder, confirm the presence of the required structure for oxygen conduction [4].

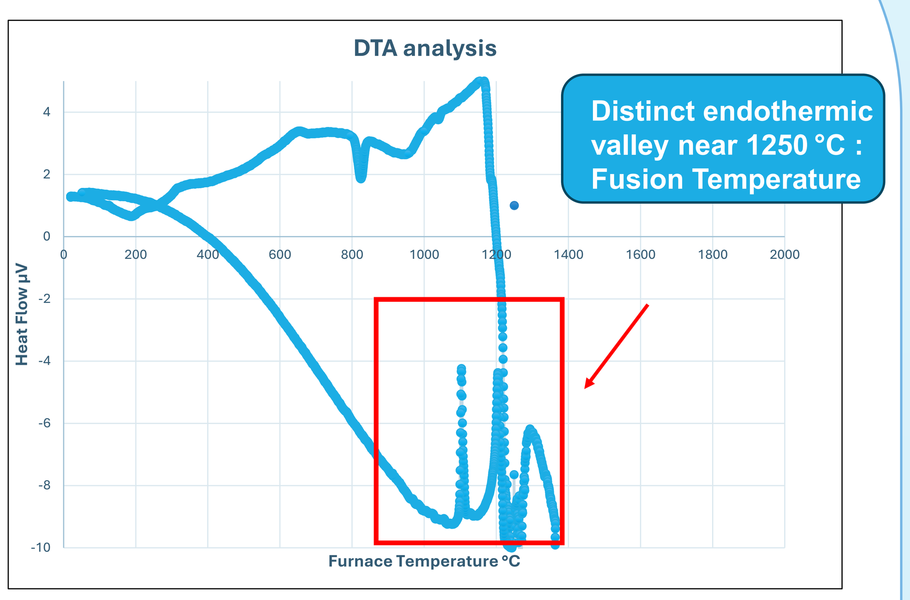

Figure 11 – DTA (Differential temperature analysis) of BSCF sample.

A prototype of the DBD reactor, integrated with the ceramic membrane, is constructed according to fig 13. The membrane is glued to the quartz tube with a ceramic adhesive, on a ceramic base commissioned for this purpose.

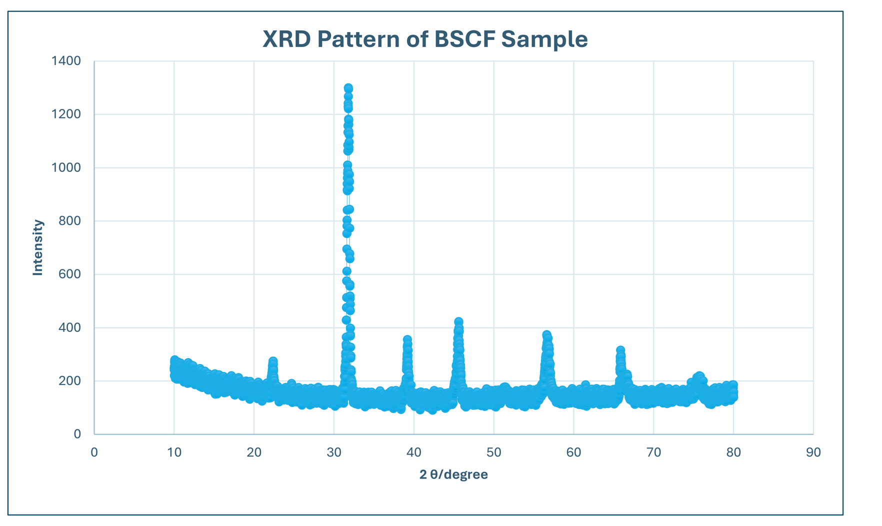

Figure 12 – XRD analysis of a BSCF sample, showing a typical perovskite structure.

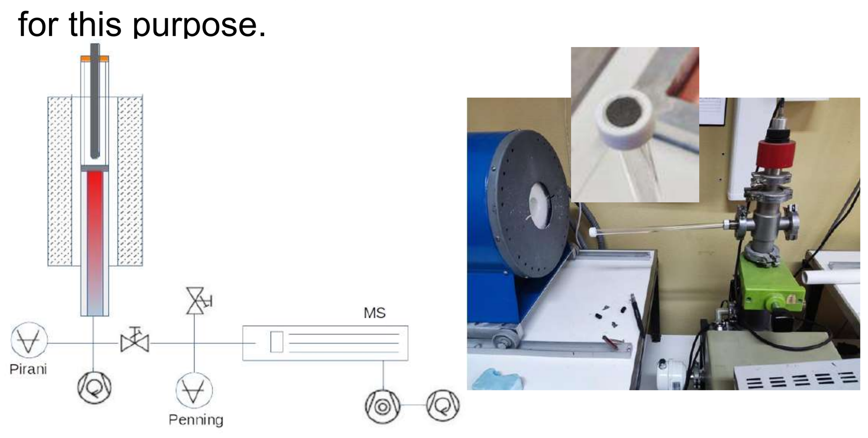

Figure 13 – Reactor prototype and set-up.

- Structural and chemical SEM analysis reveals:

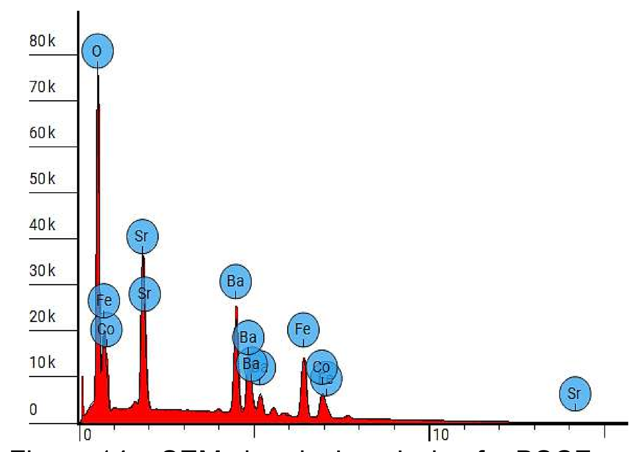
Figure 14 – SEM chemical analysis of a BSCF sample.

Multi-step heating cycle of 30 h

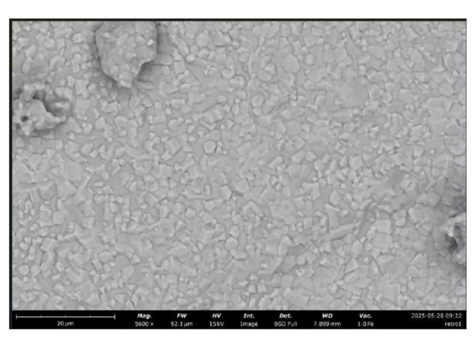

Heating cycle of 15 h, 1100 °C

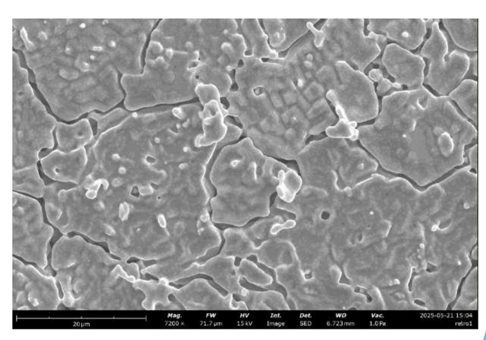

- Improved structural integrity and compactness with a multi-step heating cycle, due to oxygen reabsorption;
- Highly porous structure at 15 h due to oxygen deficiency, resulting in poorer stability.

Conclusions

The work presented highlights the various steps of the design and development of a DBD plasma reactor for the conversion of CO_2, coupled with the mixed ionic-electronic properties of perovskite-based membranes for oxygen retrieval. 2D and 3D reactor models, depicting reactor operation through finite element simulations, show an overall good agreement as depicted in fig 15. Irregularities are found due to the complexity of the 3D simulation, which earns a weaker resolution. A full chemical and structural analysis of BSCF samples was able to verify that the reabsorption of oxygen during calcination reflects in structural changes, and that the chosen experimental conditions result in the desired perovskite structure, ideal for oxygen transport. These findinds offer benchmark work for the development of an integrated system to produce oxygen as a value-added product of CO_2, conversion.

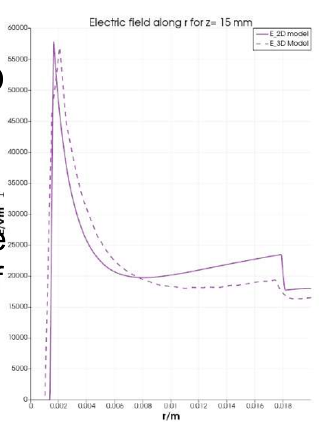
Figure 15 – 2D and 3D model comparison.

References

[1] Chen, G., Feldhoff, A., Weidenkaff, A., Li, C., Liu, S., Zhu, X., Sunarso, J., Huang, K., Wu, X., Ghoniem, A. F., Yang, W., Xue, J., Wang, H., Shao, Z., Duffy, J. H., Brinkman, K. S., Tan, X., Zhang, Y., Jiang, H., ... Kriegel, R. (2021). Roadmap for Sustainable Mixed Ionic-Electronic Conducting Membranes. Advanced Functional Materials, 32(6). https://doi.org/10.1002/adfm.202105702

[2] Huang, B. (2011). *Thermo-Mechanical Properties of Mixed Ion-Electron Conducting Membrane Materials* (*Energie & Umwelt / Energy & Environment*, Band 124). Jülich, Germany: Forschungszentrum Jülich. ISBN 978-3-89336-746-7.

[3] W. Schafbauer, R. Kauert, N.H. Menzler, H.P. Buchkremer, Tape casting of anode substrate for SOFCs. CD-ROM Proc. of the 8th Europ. SOFC Forum, Poster B0512, 30.06-04.07.2008, Lucerne, Switzerland.

[4] Singh, M. et al. (2017). "Synthesis and characterization of perovskite barium titanate thin film and its application as LPG sensor". In: Sensors and Actuators B: Chemical 241, pp. 1170–1178. DOI: 10.1016/j.snb.2016.10.018. URL: https://doi.org/10.1016/j.snb.2016.10.018

10/09/2025